Experimental optimization of an innovative biogas upgrading process adapted to the agricultural context

Valentin Fougerit, Julien Lemaire, Marc-André Theoleyre, Moncef Stambouli

EXPERIMENTAL OPTIMIZATION OF AN INNOVATIVE BIOGAS UPGRADING PROCESS ADAPTED TO THE AGRICULTURAL CONTEXT

Fougerit V., Lemaire J., Théoleyre M.-A., Stambouli M.
Department of Chemical Engineering and Materials, CentraleSupélec, Université de Paris-Saclay
SFR Condorcet FR CNRS 3417
Centre Européen de Biotechnologie et de Bioéconomie (CEBB), 3 rue des Rouges-Terres, 51110 Pomacle, France
+33 6 81 92 84 22
valentin.fougerit@centraliens.net

ABSTRACT: The development of the large European biomethane potential is facing the challenge of the biogas upgrading technologies adaptation to the agricultural context (small and medium size anaerobic digestion units, rural environment). Membrane contactors are an opportunity to adapt the robust Water Scrubbing (WS) process and to decrease the high specific investment costs reported for available technologies. Microporous polypropylene (PP) hollow fiber membrane contactors were combined in an absorption/desorption closed-loop using water as the absorbent. A Design of Experiments methodology highlighted the gas and liquid flowrates, the inlet biogas composition and the absorption gas pressure to be the most significant parameters impacting biomethane quality with a low level of interactions. From the subsequent optimization, gas-grid quality biomethane ($y_{CH_4}^{out} = 97.6\%$) was produced with a moderate recovery rate ($R_{CH_4} = 83.7\%$). The limited mass transfer efficiency may be compensated by a larger membrane area. Alternatively, the addition of a methane recycling loop, similarly to the conventional WS process, significantly improved the methane recovery rate ($y_{CH_4}^{out} = 95.9\%$ / $R_{CH_4} = 93.5\%$). These experimental results were confirmed by on-site upgrading of raw farm biogas.
Keywords: upgrading, methane, absorption, membrane contactor, process intensification.

1 INTRODUCTION

In the last decades, biogas has been considered as an energy source to build a sustainable energy mix and substitute fossil fuels. The Anaerobic Digestion (AD) of organic matter (agricultural waste, industrial waste, bio-waste, sewage sludge, energy crops…) produces biogas essentially composed of methane and carbon dioxide [1]. Its calorific content can be converted through several pathways: heat production, electricity production or conversion to biomethane [2]. The latter offers a substitute to fossil natural gas: it can be stored and transported in the gas-grid infrastructure and/or utilized as vehicle fuel [3].

Several processes are available for biogas upgrading and relies on different separation principles [4], [5]: gas-liquid absorption (physical such as water or organic scrubbing, chemical such as amine scrubbing), adsorption (PSA), gas membrane permeation or cryogeny. Among them, Water Scrubbing (WS) offers the advantages of a chemical-free process with a limited energy consumption $0.212\ kWh.Nm_{biogas}^{-3}$ [6]. Its robustness is well-adapted to the agricultural context with non-technician operators [7], [8]. These technologies aim at producing a gas-grid quality biomethane ($y_{CH_4}^{out} > 97\%$ for H gas in France) with the highest methane recovery rate R_{CH_4} (generally above 97%).

Europe and France specifically hold a massive potential for biomethane production [9], [10]. Within it, agricultural waste from small and medium size farms represent a significant share [11]. Though, the development of biogas upgrading technologies is limited due to their rising specific investment costs as the size of the AD unit decreases [5]. Gas permeation and WS are the leading technologies on this specific market. WS is particularly adapted to a rural context due to its tolerance to biogas impurities (such as volatile organic compounds or hydrogen sulfide).

Hollow fiber membranes, a technology derived from the artificial lung technology, is a gas-liquid contacting device which offers several advantages [12], [13]. Its modular nature offers an easy process design while its compactness makes it visually more attractive than conventional packed columns. The hydrophobic membrane confines both gas and liquid phases to their respective compartments and provides an operational flexibility (no flooding or channeling issues).

As another advantage, the use of membrane contactors in both absorption and desorption steps avoids the depressurization of the solvent generally needed for air stripping desorption occuring in packed columns; this represents a significant energy saving as the solvent recompression is considered to account for 20-30% of the process energy requirement [14].

These advantages make it an attractive solution for gas-liquid absorption processes. Most of the studies focused on post-combustion carbon capture [12]–[16] but a few of them experimentally explored its potential for biogas [17]–[21] or natural gas upgrading [21]–[24]. The largest membrane areas reported were tested with PP hollow fibers (highly available for processability and cost considerations).

The mass transfer resistance is typically described by a resistance in serie model divided into the gas, membrane and liquid phases [25]. In the case of pure CO_2 absorption, the limiting mass transfer resistance was demonstrated to be located in the liquid phase [25], [26]. Similarly, in the case of biogas upgrading, McLeod proved that the carbon dioxide absorbed flow $Q_{CO_2}^{abs}$ in water was driven by the liquid velocity when a physical absorbent was used [17]. Considering only absorption, 85% biomethane was produced but the methane slip was already significant ($R_{CH_4} = 94.78$ %). Using a 1M NaCl solution instead of pure water, R_{CH_4} was increased to 96.00 % thanks to the salting out effect. In a process development perspective, only one recent study carried out experimental work to implement an absorption/desorption cycle applied to biogas upgrading, as presented by Teplyakov [27]. With water as the absorbent, Kim produced a gas-grid quality biomethane ($y_{CH_4}^{out} = 98\%$) though with a lower recovery rate ($R_{CH_4} = 85$ %) [18]. Coupling absorption and

desorption steps, R_{CH_4} was further decreased to 75%. Despite biogas upgrading standards were not reached, the process potential was confirmed by a stability over 50h.

The main concern regarding the industrial application of hollow fiber membrane modules to gas-liquid absorption processes is the membrane wetting phenomenon [28]. Pores of the hydrophobic membrane are partially filled with solvent, thus increasing the membrane mass transfer resistance. Absorbed CO_2 flux was divided by 2 after 800 hours of operation with 30%wt monoethanolamine (MEA) solution [15]. The overall mass transfer resistance was increased by 21-53 % in the case of pure CO_2 absorption in water after some hours of operation [29]. The compatibility of the solvent with the membrane material is an essential selection criterion to limit this phenomenon [30]. Current research on membrane materials is addressing this wetting issue. The deposition of a thin dense layer or the development of liquid-filled membrane are potential solutions [13], [31]. Another strategy consists in increasing the membrane hydrophobicity by membrane surface treatment [32], [33].

The results from these previous studies indicate the potentialities of hollow fiber membrane modules for biogas upgrading using water as the absorbent. This paper aims at experimentally optimizing the coupled absorption/desorption process using a liquid closed-loop. Experiments were run in a partial wet mode to account for the membrane wetting limitation. The effects of operating parameters (flowrates, pressure, inlet biogas composition) have been studied through a Design of Experiments. From these initial results, the influence of the membrane area at the absorption step was tested in an open-loop configuration. At last, a new process configuration mimicking the intermediate flash tank from the WS process with a methane recycling loop was suggested and assessed.

Table I: Geometric features of the 2.5"x8" Extra-Flow module

Parameter	Value	Source
External membrane surface	1.4 m^2	[34]
Inner radius of the fiber bundle R_i	1.10 $\times 10^{-2}$ m	[34], [35]
Outer radius of the fiber bundle R_o	2.32 $\times 10^{-2}$ m	[34]
Fiber length	0.203 m	[34], [35]
Fiber effective length l_{eff}	0.146 m	[34]
Number of fibers N_f	10 200	[35]
Specific area a	4 089 m^2/m^3	Calculated

2 EXPERIMENTAL APPARATUS

2.1 Hollow fiber membranes and modules

The membrane module was selected from a range of available industrial modules (Liqui-Cel® Extra-Flow) in order to easier the foreseen process upscaling step. The geometric features of the modules and the data on both membrane types used in this study are respectively presented in Table I and Table II. This module range is built with a diverting baffle at its center to enhance the mass transfer efficiency. As the liquid flows in the shellside, the flow pattern is in between the counter-current parallel flow and the cross-flow configurations. The fiber bundle of the 2.5"x8" module is estimated at 10 200 fibers.

The X-50 fiber shows a higher porosity compared to the X-40 type (40-45% against 20-25%) and a lower thickness (80 µm against 100). These features are likely to enhance the gas-liquid mass transfer. Thus, a X-50 module is used for the absorption step. The X-40 type is selected at the desorption step for its higher mechanical resistance: it indeed faces a 13-fold higher transmembrane pressure.

Table II: Hollow fiber membrane data from manufacturer

Parameter	X-40	X-50
Applications	Degassing of other gases	CO_2 degassing
Material	PP	PP
Inner fiber diameter	200 μm	220 μm
External fiber diameter	300 μm	300 μm
Porosity	$20-25\%$	$40-45\%$
Tortuosity	$2-3$	$2-3$
Average pore diameter	0.03 μm	0.03 μm
Maximum liquid operating pressure (for $T < 40\ °C$)	7.2 $bar\ g$	7.2 $bar\ g$

2.2 Experimental set-up for biogas upgrading

A modular set-up was designed to evaluate the biogas upgrading process with different configurations. The reference configuration used in the Design of Experiments (DoE) is detailed in Figure I. Carbon dioxide from biogas is dissolved into reverse osmosis water in the absorption module. The CO_2-rich liquid is then degassed by applying a vacuum in the desorption module. Vacuum is preferred to air stripping firstly to avoid air traces in the outlet biomethane but also to produce a non-diluted offgas stream. The vacuum pump (Vacuubrand MZ 2C NT VARIO) establishes a pressure level in the range 50-500 mbar a.

The inlet gas flowrate and its composition are controlled by a 2-way mixer equipped with mass flow controllers (FC 41 and FC 42, Bronkhorst In-Flow CTA, ± (1 %RD + 1 %FS)). Pure gases (CO_2, CH_4 - Air Liquid AlphaGaz 1 standard) were used to produce synthetic mixtures. After CO_2 removal, the outlet gas flowrate is measured in another mass flow controller (FC 43, Bronkhorst Low-ΔP-Flow, ± 1 %FS). The process gas pressure is regulated with a PID controller connected to the solenoid valve of the outlet mass flow controller. The degassed gas flow, named offgas, is measured in a mass flowmeter (Bronkhorst In-Flow CTA, ± (1 %RD + 1 %FS)). It takes about 5 minutes for the gas flows and pressure to stabilize at their setpoints. As mass flowmeters were calibrated using air, they require the use of corrective factors depending on gas composition analysis which induce an additional uncertainty $\pm 2\%$.

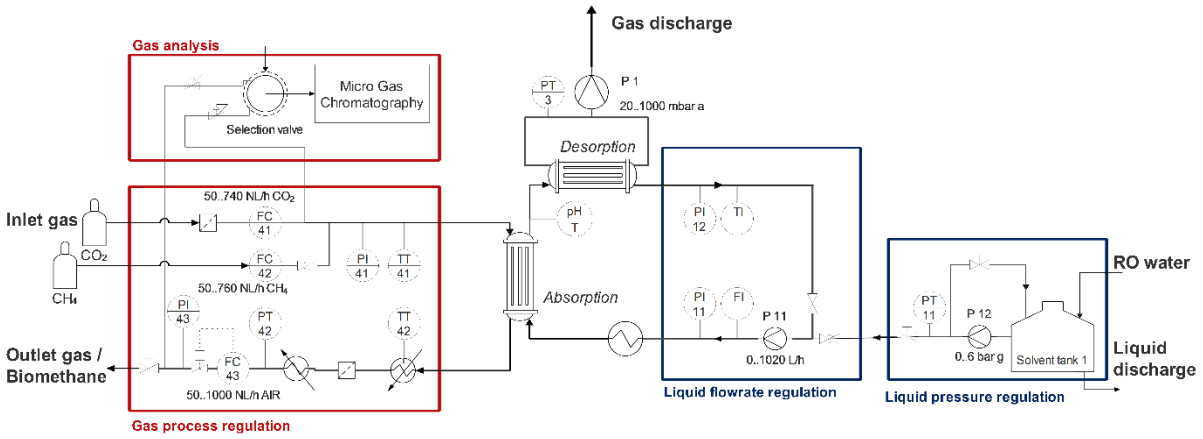

Figure I: Process flow diagram for the reference process architecture

Gas composition are analysed at the inlet, biomethane outlet and offgas outlet with an Agilent 490 micro Gas Chromatography (micro-GC) equipped with a thermal conductivity detector (TCD) detector. O_2, N_2 and CH_4 are separated on a 10m Molsieve 5Å column while CO_2 is separated on 10m PoraPLOT U. The micro-GC equipment was combined with a flow-through selection valve (VICI 6-streams selector valve). The pressure of the biogas inlet and biomethane outlet samples are regulated below 1 bar g to comply with micro-GC specifications. 4 standard gases are used for calibration. Due to the combination of the error from the gas sampling system, the calibation error, the analytical repeatability and the analytical precision, the analytical error is estimated to $\pm 0.3\%\ vol.$.

The liquid flow was operated in a closed-loop configuration during DoE. Two pumps are respectively regulating the pressure and the flowrate. They are controlled by a pressure transmitter PT 11 and a vortex flowmeter FI (Liqui-View) through frequency converters. Liquid pH is measured in a flow-through fitting positioned after CO_2 absorption step (Mettler-Toledo InPro 4262i).

The DoE investigated the available operating conditions range presented in Table III.

Table III: Range of the operating conditions

Operating parameter	Range	Unit
$\mathbf{P_g}$	0 – 7	$bar\ g$
$\mathbf{Q_{CO_2}}$	74 – 739	$NL.h^{-1}$
$\mathbf{Q_{CH_4}}$	76 – 530	$NL.h^{-1}$
$\mathbf{P_l}$	0 – 8	$bar\ g$
Water flowrate $\boldsymbol{Q_l}$	30 – 240	$L.h^{-1}$

2.3 Data treatment

Experimental results are compared according to two key performance indicators: the biomethane quality $y_{CH_4}^{out}$ and the methane recovery rate R_{CH_4}. The process is evaluated in its steady state regime. Gas composition analyses were performed 20 minutes after the process parameters reached their setpoints. Similar stabilization times are reported in the literature [17], [18]. A second gas composition analysis was performed 15 minutes after the first one to confirm the steady state regime had been reached.

The methane recovery rate R_{CH_4} can be derived from inlet and outlet gas flowrates and compositions (Eq. 1).

$$R_{CH_4} = \frac{Q_{CH_4}^{out}}{Q_{CH_4}^{in}} = \frac{y_{CH_4}^{out} Q^{out}}{y_{CH_4}^{in} Q^{in}} \qquad \text{Eq. 1}$$

Though, the uncertainties are stronger on the gas flowrates than on the gas composition analysis. Therefore, a method based on the composition of the three gas flows was preferred. The combination of two mass balances (total gas and methane only) leads to:

$$R_{CH_4} = \frac{y_{CH_4}^{out}}{y_{CH_4}^{in}} \frac{\left(y_{CH_4}^{in} - y_{CH_4}^{off}\right)}{\left(y_{CH_4}^{out} - y_{CH_4}^{off}\right)} \qquad \text{Eq. 2}$$

The efficiency of the CO_2 mass transfer is assessed for the open-loop experiments. First, the logarithmic mean of the transfer potential Δx_{ML} is calculated.

$$\Delta x_{ML} = \frac{\left(x^{out,*} - x^{out}\right) - \left(x^{in,*} - x^{in}\right)}{\ln\left(x^{out,*} - x^{out}\right) - \ln\left(x^{in,*} - x^{in}\right)} \qquad \text{Eq. 3}$$

$x^{out,*}$ and $x^{in,*}$ are derived from gas composition analysis and values from Henry coefficients [36]. x^{out} is calculated by a CO_2 mass balance over the absorption unit (Eq. 4). x^{in} is reasonably assumed to be zero in the open-loop configuration (initially gas-free inlet absorbent).

$$x_{out} = \frac{G_{in}}{L} y_{CO_2}^{in} - \frac{G_{out}}{L} y_{CO_2}^{out} \qquad \text{Eq. 4}$$

A constant liquid overall mass transfer coefficient K_L^0 is then derived from experimental data. It is related to K_L coefficient expressed in $m.s^{-1}$ by Eq. 6.

$$K_L^0 = \frac{L(x_{out} - x_{in})}{a\ \Delta x_{ML}\ SZ} \qquad \text{Eq. 5}$$

$$K_L = \frac{K_L^0}{c_{tot}^l} \cong \frac{K_L^0}{c_{H_2O}^l} \qquad \text{Eq. 6}$$

3 DESIGN OF EXPERIMENTS

3.1 Influence of process parameters

In a first approach, the process parameters and their expected influence on the performances have been summarized in Table IV. The flows Q_g and Q_l are the main parameters of the gas-liquid absorption processes, typically described by their ratio Q_g/Q_l. The gas pressure

Table IV: Expected influence of process parameters

Parameter	Influence	$y_{CH_4}^{out}$	R_{CH4}
Q_g	Increase the CO_2 flow to be removed	-	+
Q_l	Increase the potential gas removal both for CO_2 and CH_4	+	-
P_g	Decrease the partition coefficient m, thus the liquid potential gas removal is increased	+	-
P_l	Increase the membrane wetting and consequently the mass transfer resistance [37]	-	+
P_{vac}	The lower the pressure at desorption, the higher the mass transfer potential to regenerate the absorbent	-	+
T_g	Influence of gas temperature is not known but likely not to be significant	?	?
T_l	A lower temperature enhances the absorption capacity [36]	+	-
$y_{CH_4}^{in}$	Lower the CO_2 flow to be removed Decrease the CO_2 mass transfer potential $(x^* - x)$	+	-

at absorption P_g and the liquid temperature T_l impact the gas-liquid equilibrium (i.e. the partition coefficient m). According to Henry's law, the liquid pressure P_l has no impact on this equilibrium. Its impact on the gas absorption process is found through the increase of transmembrane pressure. Indeed, membrane wetting is a limitation to mass transfer which is enhanced by a high transmembrane pressure. A low vacuum level P_{vac} applied at the desorption step increases the mass transfer potential. Therefore, a more efficient solvent regeneration is expected.

The inlet gas composition $y_{CH_4}^{in}$ necessarily impacts the process performances. At industrial scale, the biogas quality is an input parameter which depends on the substrates and on the AD process.

Among the listed parameters, five are selected for further investigation for their supposed influenced on the biogas upgrading process: both gas and liquid flowrates Q_g and Q_l, gas absorption and vacuum pressures P_g and P_{vac}, and inlet biogas composition $y_{CH_4}^{in}$.

3.2 Design of Experiments

The DoE methodology was adopted to compare the relative influence of the process parameters and their interactions in a range of operating conditions. Five parameters were selected and three levels were defined to investigate the quadratic influences and interactions (Table V). The temperature of the absorbent was measured but not regulated ($T_l = 25°C \pm 3°C$). Biomethane quality $y_{CH_4}^{out}$ was the selected process response for its low uncertainty ($\pm 0.3\%\ vol.$).

A central composite design was used to reduce the number of experiments (243 tests initially). The central composite design is divided in 3 matrix:

- A factorial design with 2 levels (-1 and +1): 32 tests;
- A series of tests at the center of the domain: N_0 tests;
- A series of tests on the axis of the domain (-θ and +θ for each parameter): 10 tests.

The value of θ=2.378 is chosen from tabulated values to satisfy the optimality criteria: rotability, orthogonality and uniform precision. The criteria of orthogonality and uniform precision cannot be satisfied at the same time. Therefore, the design is qualified of quasi-orthogonal.

For a given number of parameters (here k = 5), the number of tests N_0 at the center of the domain is defined according to the criterion that must be satisfied (17 and 10 respectively for orthogonality and uniform precision criteria). In practice, 15 tests were performed at the center of the domain.

3.3 Statistical processing

A quadratic model with interactions was used to interpret the experimental data. Three models are successively constructed in a MATLAB program:

- Model1 which is the raw model with all the coefficients considered;
- Model2 which is model1 with only the same significant coefficients conserved;
- Model3 which is an optimization of the coefficients with the significant parameters only.

To determine whether the effect of the parameter is significant, the ratio of its effect a_{P^i} against the model standard error s_{model} is compared to a Student law coefficient with $N - C$ degrees of freedom (N number of experiments, C number of coefficients in the model).

$$\left|\frac{a_{P^i}}{s_{model}}\right| > t_{1-\alpha/2,(N-C)}^{student} \quad \text{Eq. 7}$$

The value of α determines the confidence interval. $\alpha = 0.05$ is a typical choice which describes the confidence interval at 95 %.

The same student coefficient and the mean squared error σ_{model} determines the precision of the model P_{model} by:

$$P_{model} = t_{1-\alpha/2,(N-C)}^{student} \cdot \sqrt{\sigma_{model}} \quad \text{Eq. 8}$$

3.4 Data rejection

The tests have been performed at different time periods by two different operators, with membranes subject to degradation. To perform an efficient statistical analysis, systematic mass balances (total gas, methane and carbon dioxide) have tested the result consistency. The mass balance errors were calculated according to:

$$\varepsilon_{tot} = \frac{Q_{out} + Q_{off} - Q_{in}}{Q_{in}} \quad \text{Eq. 9}$$

$$\varepsilon_i = \frac{y_i^{out} Q_{out} + y_i^{off} Q_{off} - y_i^{in} Q_{in}}{y_i^{in} Q_{in}} \quad \text{Eq. 10}$$

Most of the experiments display a very good mass balance ($\varepsilon < 5\%$) for the three indicators (Figure II). In such a process, a 15% error can even be considered admissible. As a general trend, the CH_4 and CO_2 errors

Table V: Definition of parameters' levels for the Design of Experiments

Level	Q_l $[L.h^{-1}]$	Q_g $[NL.h^{-1}]$	P_g $[bar\ g]$	P_{vac} $[mbar\ a]$	$y_{CH_4}^{in}$ $[\%vol.]$
Parameter	P1	P4	P3	P2	P5
-θ	60	205.0	1.10	100.0	30.0
-1	103.5	355.7	2.2	157.9	47.4
0	135	465.0	3.0	200.0	60.0
+1	166.5	574.3	3.8	242.1	72.6
+θ	210	725.0	4.90	300.0	90.0

tend to be positive and negative respectively. At the end of the campaign, a batch of tests has a stronger CO_2 error (10 – 25 %). These tests are performed at the extremity of the parameter axis. Three of these tests had replicates with a better mass balance. Therefore, no experiment with a mass balance error over 15% was integrated in the statistical analysis.

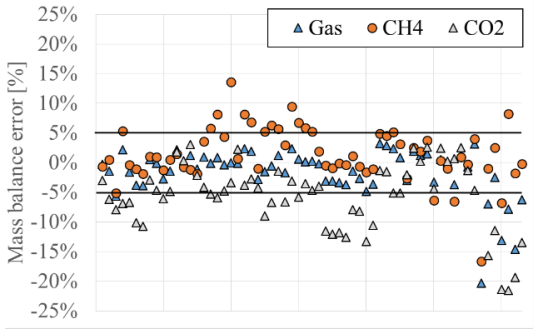

Figure II: Mass balance errors on the DoE experiments

3.5 Results

The residual distribution of the quadratic model with interactions fits a normal density function (Figure III): the error is randomly distributed within the domain. Moreover, no deviation of these residuals were observed neither with the experiment order nor with the measured response. The analysis of the model response in Figure IV shows that the model is in agreement with the measured response in a 95% confidence interval. The precision is though limited to $P_{model} = \pm 4.0\%$ (Eq. 8).

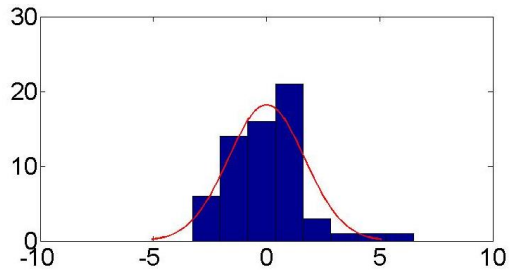

Figure III: Residuals distribution for the methane content response (quadratic model with interactions)

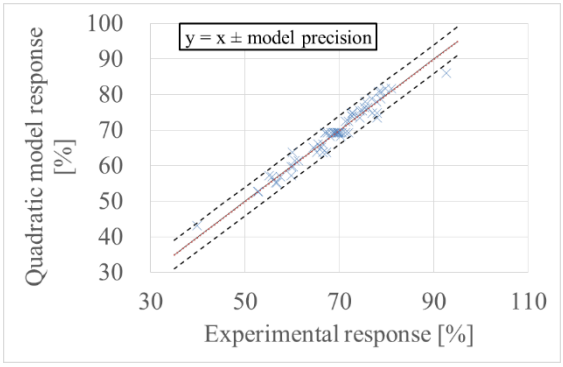

Figure IV: Model response against measured response and 95% confidence interval

Most of the experimental results are concentrated in the range $y_{CH_4}^{out} = 55 - 80\%$ which is below the targeted biomethane quality ($y_{CH_4}^{out} > 97\%$). The only experiment with a recorded biomethane quality above 90% ($y_{CH_4}^{out} = 92.6\ \%$) is not in the confidence interval of the model. It means that the model resulting from statistical analysis may not describe well the process performances in the targeted domain.

The observed effects of the process parameters displayed in Figure V are in accordance with the preliminary discussion in section 3.1. Only the pressure P_{vac} applied at the desorption step is not found to be significant in the domain ($100 - 300\ mbar\ a$). The inlet biogas quality is strongly significant both in the first order, the second order and by its interactions with other parameter (Q_l And P_g). This finding means that the process performances is highly dependent on the inlet biogas quality $y_{CH_4}^{in}$. The flowrates have limited quadratic effects: the gas flowrate quadratic effect Q_g is almost not significant ($a_{\cdot P5^2} = 0.39$). This other important result indicates that both parameters can be aggregated into the Q_g/Q_l ratio for next experimental campaigns. In order to optimize the biomethane quality, P_g must be set high while the Q_g/Q_l ratio must be low.

From the DoE findings, process parameters were varied to produce the targeted biomethane quality in a liquid closed-loop configuration. For a given gas flowrate ($Q_g = 153$ NL.h^{-1}), a Q_g/Q_l ratio of $1.30\ NL.L^{-1}$ produced biomethane ($y_{CH_4}^{out} = 97.6\%$) with a methane recovery rate R_{CH_4} of 77.6%. A higher Q_g/Q_l ($1.69\ NL.L^{-1}$) was still fulfilling the quality requirement with an improved recovery rate ($R_{CH_4} = 83.7\%$).

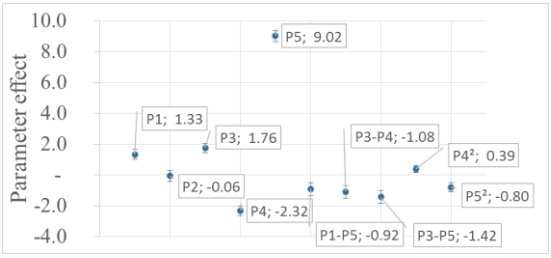

Figure V: First order effects and significant second order parameters from the quadratic model

The recovery rate are still low compared to the available technologies which allow to recover more than 97% of the inlet methane flow [4], [5]. Nonetheless, this experimental set-up produces on one side a methane-rich fraction which can be injected into the gas grid, and on the other side a CO_2-rich fraction. Compared to other available technologies, this offgas flow is not diluted in an air flow (as for air stripping) and still contain a significant methane fraction (respectively $y_{CH_4}^{off} = 25.3\ and\ 20.0\%$). This methane content is high enough to burn this offgas flow in a low calorific burner and cover the digester heat demand. This process point is thus a first proof-of-concept for a biogas upgrading process of industrial interest.

4 STRATEGIES FOR PROCESS IMPROVEMENT

4.1 Limitation in the DoE experiments

The DoE confirmed the gas-to-liquid ratio to be a significant parameter to adjust the process performances. To further investigate the role of this aggregated parameter, the response of the DoE model was plotted against the performances of an ideal mass transfer exchanger (liquid outlet at equilibrium with inlet biogas) in Figure VI. The inlet biogas composition was set to a typical biogas composition ($y_{CH_4}^{in} = 60\%$) and the absorption pressure was maximised to $P_g = 5\ bar\ g$ in order to improve the biomethane quality.

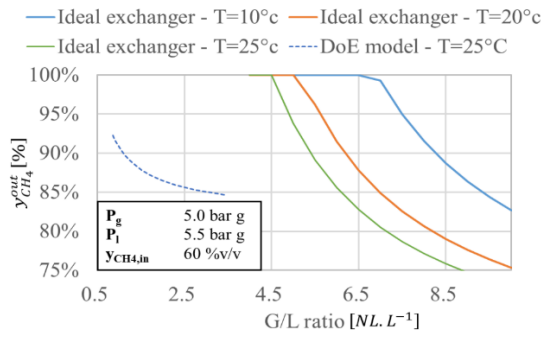

Figure VI: Influence of Q_g/Q_l ratio on the biomethane quality: comparison of the DoE quadratic model with ideal exchanger performances
DoE model is applied with $Q_g = 205\ NL.h^{-1}$

In an ideal exchanger, a decrease in the water temperature improves the absorption performance. It is a way towards process intensification. Under $T_l = 20°C$, a theoretical Q_g/Q_l ratio of 5.29 $NL.L^{-1}$ is needed to obtain a 97% quality biomethane. The DoE model built from experimental data reaches 90% biomethane quality only for ratios below $1.10\ NL.L^{-1}$. It is well below the performances of an ideal exchanger.

Two hypothesis are possible explanations to this observation. Firstly, the process was operating in a closed-loop configuration. As a result, the inlet absorbent may not be fully regenerated before entering the absorption module. On the contrary, the ideal exchanger curves suppose that the inlet liquid is free of dissolved gases. The second assumption is that the experimental set-up used in the DoE campaign (i.e. a X-50 absorption module) is limited by mass transfer and therefore cannot meet the performances of an ideal exchanger. An increase of the exchange surface would improve the process performances. The second hypothesis is tested in the following paragraph.

4.2 Influence of the absorption surface

According to the transfer unit methods, a longer exchanger leads to an improved biomethane quality. Therefore, two membranes modules were set in series to double the exchange surface and test the mass transfer limitation hypothesis. An open-loop configuration was set to avoid the question of the desorption efficiency.

The biomethane quality increases by 10-15 points when the exchange surface is doubled (Figure VII) but conserves the dependency on the Q_g/Q_l ratio. These results are compared to simulated results from a 1D model describing both CO_2 and CH_4 absorption. The constant overall mass transfer coefficient K_L is an adjustable parameter of the 1D model. The adjusted K_L is not constant between the two series but still in the same range ($1.9 \times 10^{-5}\ m.s^{-1}$ and $2.5 \times 10^{-5}\ m.s^{-1}$ respectively for one and two membrane modules).

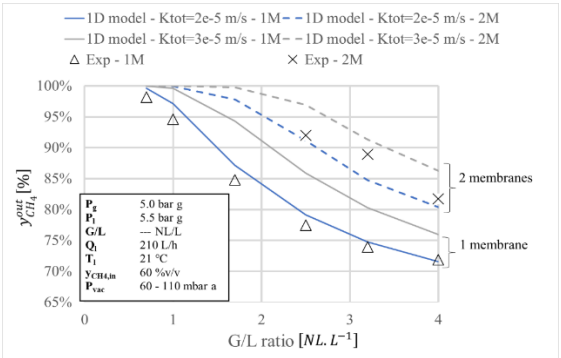

Figure VII: Comparison of biomethane quality at different Q_g/Q_l ratio with one or two membrane modules *Open-loop configuration*

The adjusted values of the model are consistent with the overall mass transfer coefficient derived from the calculation of the average mass transfer potential by Eq. 5 (Table VI). The overall mass transfer coefficient relative to the gas phase is very slightly below literature values ($2.4 - 4.0\ 10^{-5} m.s^{-1}$ as reported by Lu [38]). K_L is constant for the 1-module serie ($2.02 \pm 0.07\ 10^{-5} m.s^{-1}$). It slightly increases during the 2-module serie and a higher standard deviation is observed ($2.80 \pm 0.19\ 10^{-5} m.s^{-1}$).

The increase of the membrane area could improve the biomethane composition. Though, simulations from the 1D model indicates that 7 membrane modules in series

Table VI: Overall mass transfer coefficients calculated from experimental data

N modules	Q_l $[L.h^{-1}]$	Q_g/Q_l $[NL.L^{-1}]$	P_g $[bar\ g]$	$y_{CH_4}^{in}$ $[\%vol.]$	K_L $[10^{-5}m.s^{-1}]$	K_G $[10^{-5}m.s^{-1}]$
1	210	0.7	5.0	60.1	2.02	1.85
	210	1.0	5.0	60.0	2.02	1.85
	210	1.7	5.0	59.8	1.96	1.80
	210	2.5	5.0	59.9	1.94	1.78
	210	3.2	5.0	60.0	1.99	1.80
	210	4.0	5.0	60.0	2.15	1.92
2	210	2.5	5.0	59.8	2.58	2.38
	210	3.2	5.0	60.3	3.03	2.73
	210	4.0	5.0	60.0	2.81	2.59

are required to reach the targeted biomethane quality ($y_{CH_4}^{out} > 97\%$) under $Q_g/Q_l = 4.0\ NL.L^{-1}$. This ratio was chosen to be slightly below the ratio needed in the case of an ideal mass exchanger (Figure VI). Moreover, the inlet liquid is supposed to be free from dissolved gas content.

The important number of modules is explained by a reduced average absorbed CO_2 flux J_{CO_2}. Figure VIII shows that this flux is reduced by 20 % from the 1-module serie to the 2-module serie. In the second module, CO_2 has already been largely removed from the gas flow and therefore the mass transfer potential is lower than in the 1-module serie. In the membrane-wet regime, similar fluxes were reported for the absorption of pure CO_2 under atmospheric pressure in water ($0.9 - 1.4\ 10^{-3}\ mol.m^2.s^{-1}$) [29].

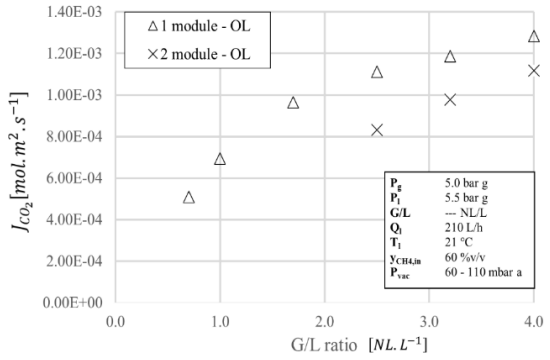

Figure VIII: Absorbed CO_2 flux at different Q_g/Q_l ratio with one or two membrane modules

Open-loop configuration

4.3 Addition of a methane recycling loop

The impact of the Q_g/Q_l ratio was highlighted both from DoE findings and from Figure VII. The biomethane quality is improved with a lower Q_g/Q_l ratio: it reaches $y_{CH_4}^{out} = 94.6\%$ under $Q_g/Q_l = 1.00\ NL.L^{-1}$. In the meantime, the methane recovery rate decreases ($R_{CH_4} = 84.2\%$ under $Q_g/Q_l = 1.00\ NL.L^{-1}$). A new process arrangement is suggested and assessed to minimize this methane slip.

Commercial biogas water scrubbers are designed with an intermediate step for the regeneration of the CO_2-rich solvent. A flash-tank is set to decrease the pressure at an intermediate level in order to recycle part of the dissolved methane content [6]. A new membrane contactor was therefore added in the liquid closed-loop to mimic this architecture (Figure IX).

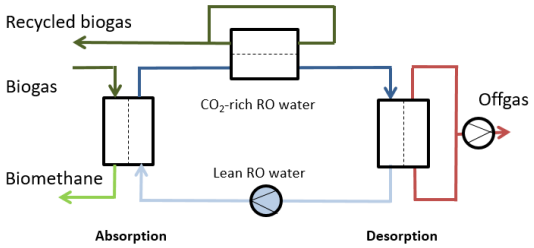

Figure IX: Simplified closed-loop configuration with methane recycling loop

The process performances were compared against the results obtained in the reference architecture (Figure I) under the same operating conditions. The recycled flow was controlled by a needle valve to investigate the influence of the gas pressure in the intermediate membrane contactor. The biomethane quality was maintained constant ($y_{CH_4}^{out} = 95.5 - 95.9\%$) and comparable to the methane content obtained in the reference case (Figure X). By progressively closing the needle valve, the intermediate gas pressure P_{int} increased from 0.25 to 1.9 $bar\ g$. It increased the methane content in the recycled gas flow $y_{CH_4}^{rec}$ from 57.2 to 76.9 %.

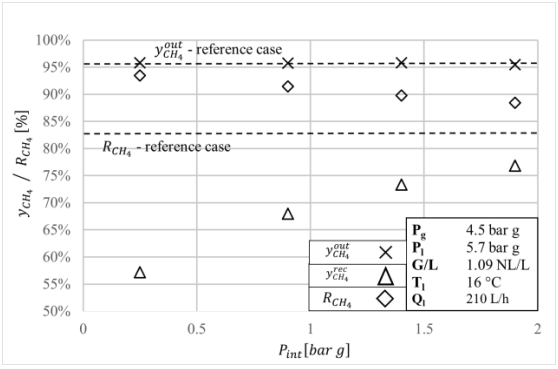

Figure X: Addition of methane recycling loop: influence of intermediate gas pressure

The methane recovery rate R_{CH_4} was calculated by Eq. 2 assuming that the recycled gas flow would be mixed with process inlet biogas flow. Indeed, the methane content in the recycled gas flow would not significantly affect the inlet biogas quality ($y_{CH_4}^{in} = 60\%$). R_{CH_4} thus decreased from 93.5 to 88.5% with the increase of P_{int}. As P_{int} increases, the recycled gas flow

Table VII: Overall mass transfer coefficients calculated from experimental data
Reference configuration

Biogas	Q_l $[L.h^{-1}]$	Q_g/Q_l $[NL.L^{-1}]$	P_g $[bar\ g]$	T $_l$ $[°C]$	$y_{CH_4}^{in}$ $[\%vol.]$	y_{air}^{in} $[\%vol.]$	K $_L$ $[10^{-5}m.s^{-1}]$	$y_{CH_4}^{out}$ $[\%vol.]$	R $_{CH4}$ [%]
Synth.	120	1.30	5.0	27.0	59.5	0.0	2.62	97.6	77.6
	90	1.69	5.0	26.7	59.7	0.0	2.85	97.2	83.7
Raw	210	1.09	4.5	16.3	59.0	1.8	3.07	94.3	83.9
	210	1.09	4.5	16.2	58.0	0.8	2.92	96.2	82.8

is reduced, resulting in an increased methane slip at the desorption step. Completely closing the intermediate needle valve would stop the methane recycling and the process configuration would be similar to the reference case ($R_{CH_4} = 83\%$).

The best process performances ($y_{CH_4}^{out} = 95.9\%$ / $R_{CH_4} = 93.5\%$) were obtained at low intermediate pressure $P_{int} = 0.25\ bar\ g$. The corresponding overall mass transfer coefficient is slightly below previous results in reference configuration ($2.53 \times 10^{-5}\ m.s^{-1}$). It indicates that the addition of the recycling loop mainly impacts the methane mass transfer.

4.4 On-site experimental campaign with farm biogas

These results obtained with synthetic biogas had to be confirmed during an on-site experimental campaign to upgrade real raw biogas. The farm AD unit co-digests cow slurry with agroindustrial waste (beet pulp, brewing dregs…), crop residues or grass silage. A by-pass flow is diverted from the average 30 $Nm^3_{biogas}.h^{-1}$ flow to be upgraded in the pilot process. During the 2-week field campaign, the methane content was stable ($y_{CH_4}^{in} = 56.3 - 59.0\%$). An air injection inside the digester maintains the H_2S content low ($< 200\ ppmv$) by sulfur oxidation. Though this air injection results in the presence of nitrogen and oxygen in the biogas flow ($1.7 - 2\%$). This air injection was stopped during 3 days for the experimental campaign purpose.

From the previous values of K_L, this experimental campaign was operated with a higher inlet biogas flowrate ($Q_g = 229$ NL.h^{-1}) to intensify the pilot process to its maximum. In addition, due to biogas compressor limitations, the absorption pressure P_g was set only to 4.5 $bar\ g$. The 97% biomethane quality was almost reached with a Q_g/Q_l ratio of 1.09 $NL.L^{-1}$ (Table VII). The same experimental process point was repeated with a lower inlet air content. The biomethane quality was thus increased from 94.3 to 96.2 %.

Similar biogas upgrading performances were achieved in the reference architecture both with synthetic and raw farm biogas. The process displayed similar average mass transfer coefficients with synthetic biogas and real biogas ($2.62 - 2.85 \times 10^{-5}\ m.s^{-1}$ against $2.92 - 3.07 \times 10^{-5}\ m.s^{-1}$). The slight increase may be due to an increased liquid flowrate during farm experiments. Therefore, it is reasonable to assume that the process optimization can be carried out using synthetic biogas at the lab for the sake of convenience.

Moreover, within the 2 weeks, no significant performance degradation was observed. Therefore, the exposure of the membrane material is not extremely sensitive to the presence of biogas impurities (like H_2S or volatile organic compounds). The polymer compatibility with these impurities must be carefully study for future industrial developments.

5 CONCLUSION

The use of membrane contactors for biogas upgrading purposes was optimized in an absorption/desorption cycle with a liquid closed-loop. The reference process configuration with equivalent membrane areas for the absorption and desorption steps was optimized by a Design of Experiments. A high biomethane purity ($y_{CH_4}^{out} = 97.6\%$) was obtained with an improved methane recovery rate compared to previous reported results ($R_{CH_4} = 83.7\%$ against 75%). This moderate recovery rate is a first process point of interest as the calorific content of the non-diluted offgas flow ($y_{CH_4}^{off} = 20.0 - 25.3\%$) may be used to cover the digester heating demand in a low calorific burner. Doubling the membrane area at the absorption step proved that a significant number of modules (7) are needed to approach an ideal mass exchanger under conditions $Q_g/Q_l = 4.0\ NL.L^{-1}$ close to the theoretically optimized flowrates ratio. An alternative process arrangement mimicking the conventional WS methane recycling loop revealed a significant improvement of the methane recovery rate without affecting the biomethane quality ($y_{CH_4}^{out} = 95.9\%$ / $R_{CH_4} = 93.5\%$). This second process point is a very promising result to combine the advantages of membrane contactors and WS into an innovative biogas upgrading process. Additional studies are required to optimize the membrane area ratio between the absorption, partial and final degassing steps (set to 1:1:1 in the present study) and to meet the performances of available biogas upgrading technologies.

6 REFERENCES

[1] A. Wellinger, J. Murphy, and D. Baxter, *The biogas handbook - Science, production and applications.* Woodhead Publishing, 2013.

[2] M. Pöschl, S. Ward, and P. Owende, 'Evaluation of energy efficiency of various biogas production and utilization pathways', *Appl. Energy*, vol. 87, no. 11, pp. 3305–3321, Nov. 2010.

[3] W. M. Budzianowski and M. Brodacka, 'Biomethane storage: Evaluation of technologies, end uses, business models, and sustainability', *Energy Convers. Manag.*, Aug. 2016.

[4] L. Yang, X. Ge, C. Wan, F. Yu, and Y. Li, 'Progress and perspectives in converting biogas to transportation fuels', *Renew. Sustain. Energy Rev.*, vol. 40, pp. 1133–1152, Dec. 2014.

[5] F. Bauer, C. Hulteberg, T. Persson, and D. Tamm, 'Biogas upgrading - Review of commercial technologies', 2013.

[6] Y. Xiao *et al.*, 'CO2 Removal from Biogas by Water Washing System', *Chin. J. Chem. Eng.*, vol. 22, no. 8, pp. 950–953, Aug. 2014.
[7] P. Rotunno, A. Lanzini, and P. Leone, 'Energy and economic analysis of a water scrubbing based biogas upgrading process for biomethane injection into the gas grid or use as transportation fuel', *Renew. Energy*, vol. 102, pp. 417–432, Mar. 2017.
[8] D. Benizri, 'Epuration du biogaz à la ferme : EPUROGAS, une solution énergétique et économique d'avenir. - Etude expérimentale et modélisation d'un procédé d'absorption de dioxyde de carbone avec de l'eau sous pression à une échelle industrielle -', Université de Toulouse, 2016.
[9] D. Thrän, 'European biomethane potentials', in *Workshop on Biomethane Trade*, 2012, vol. 21, p. 2012.
[10] COWI, 'State of the Art on Alternative Fuels Transport Systems in the European Union', European Commission, Jul. 2015.
[11] AEBIOM, 'A Biogas Roadmap for Europe', European Biomass Association, Brussels, Oct. 2009.
[12] P. Luis, B. Van der Bruggen, and T. Van Gerven, 'Non-dispersive absorption for CO2 capture: from the laboratory to industry', *J. Chem. Technol. Biotechnol.*, vol. 86, no. 6, pp. 769–775, Jun. 2011.
[13] S. Zhao *et al.*, 'Status and progress of membrane contactors in post-combustion carbon capture: A state-of-the-art review of new developments', *J. Membr. Sci.*, vol. 511, pp. 180–206, Aug. 2016.
[14] E. Chabanon, B. Belaissaoui, and E. Favre, 'Gas–liquid separation processes based on physical solvents: opportunities for membranes', *J. Membr. Sci.*, vol. 459, pp. 52–61, Jun. 2014.
[15] E. Chabanon, D. Roizard, and E. Favre, 'Membrane Contactors for Postcombustion Carbon Dioxide Capture: A Comparative Study of Wetting Resistance on Long Time Scales', *Ind. Eng. Chem. Res.*, vol. 50, no. 13, pp. 8237–8244, Jul. 2011.
[16] L. Gomez-Coma, A. Garea, and A. Irabien, 'Carbon dioxide capture by [emim][Ac] ionic liquid in a polysulfone hollow fiber membrane contactor', *Int. J. Greenh. Gas Control*, vol. 52, pp. 401–409, Sep. 2016.
[17] A. McLeod, B. Jefferson, and E. J. McAdam, 'Quantifying the loss of methane through secondary gas mass transport (or "slip") from a micro-porous membrane contactor applied to biogas upgrading', *Water Res.*, vol. 47, no. 11, pp. 3688–3695, Jul. 2013.
[18] S.-J. Kim, A. Park, S.-E. Nam, Y.-I. Park, and P. S. Lee, 'Practical designs of membrane contactors and their performances in CO2/CH4 separation', *Chem. Eng. Sci.*, vol. 155, pp. 239–247, Nov. 2016.
[19] A. McLeod, B. Jefferson, and E. J. McAdam, 'Biogas upgrading by chemical absorption using ammonia rich absorbents derived from wastewater', *Water Res.*, vol. 67, pp. 175–186, Dec. 2014.
[20] W. Rongwong, S. Boributh, S. Assabumrungrat, N. Laosiripojana, and R. Jiraratananon, 'Simultaneous absorption of CO2 and H2S from biogas by capillary membrane contactor', *J. Membr. Sci.*, vol. 392–393, pp. 38–47, Mar. 2012.
[21] S. Atchariyawut, R. Jiraratananon, and R. Wang, 'Separation of CO2 from CH4 by using gas–liquid membrane contacting process', *J. Membr. Sci.*, vol. 304, no. 1–2, pp. 163–172, Nov. 2007.
[22] S. A. M. Marzouk, M. H. Al-Marzouqi, M. H. El-Naas, N. Abdullatif, and Z. M. Ismail, 'Removal of carbon dioxide from pressurized CO2–CH4 gas mixture using hollow fiber membrane contactors', *J. Membr. Sci.*, vol. 351, no. 1–2, pp. 21–27, Apr. 2010.
[23] S. A. M. Marzouk, M. H. Al-Marzouqi, M. Teramoto, N. Abdullatif, and Z. M. Ismail, 'Simultaneous removal of CO2 and H2S from pressurized CO2–H2S–CH4 gas mixture using hollow fiber membrane contactors', *Sep. Purif. Technol.*, vol. 86, pp. 88–97, Feb. 2012.
[24] N. A. Rahim, N. Ghasem, and M. Al-Marzouqi, 'Absorption of CO2 from natural gas using different amino acid salt solutions and regeneration using hollow fiber membrane contactors', *J. Nat. Gas Sci. Eng.*, vol. 26, pp. 108–117, Sep. 2015.
[25] V. Fougerit, V. Pozzobon, D. Pareau, M.-A. Théoleyre, and M. Stambouli, 'Gas-liquid absorption in industrial cross-flow membrane contactors: Experimental and numerical investigation of the influence of transmembrane pressure on partial wetting', *Chem. Eng. Sci.*, Mar. 2017.
[26] A. Mansourizadeh, 'Experimental study of CO2 absorption/stripping via PVDF hollow fiber membrane contactor', *Chem. Eng. Res. Des.*, vol. 90, no. 4, pp. 555–562, Apr. 2012.
[27] V. Teplyakov, A. Okunev, and N. Laguntsov, 'Computer design of recycle membrane contactor systems for gas separation', *Sep. Purif. Technol.*, vol. 57, no. 3, pp. 450–454, Nov. 2007.
[28] H. Kreulen, C. A. Smolders, G. F. Versteeg, and W. P. M. van Swaaij, 'Determination of mass transfer rates in wetted and non-wetted microporous membranes', *Chem. Eng. Sci*, vol. 48, no. 11, pp. 2093–2102, 1993.
[29] M. Mavroudi, S. P. Kaldis, and G. P. Sakellaropoulos, 'A study of mass transfer resistance in membrane gas–liquid contacting processes', *J. Membr. Sci.*, vol. 272, no. 1–2, pp. 103–115, Mar. 2006.
[30] S. Mosadegh-Sedghi, D. Rodrigue, J. Brisson, and M. C. Iliuta, 'Wetting phenomenon in membrane contactors – Causes and prevention', *J. Membr. Sci.*, vol. 452, pp. 332–353, Feb. 2014.
[31] L. Gomez-Coma *et al.*, 'Membrane modules for CO2 capture based on PVDF hollow fibers with ionic liquids immobilized', *J. Membr. Sci.*, vol. 498, pp. 218–226, Jan. 2016.
[32] M. A. Abdulhameed *et al.*, 'Carbon dioxide capture using a superhydrophobic ceramic hollow fibre membrane for gas-liquid contacting process', *J. Clean. Prod.*, vol. 140, pp. 1731–1738, Jan. 2017.
[33] H. J. Lee and J. H. Park, 'Effect of hydrophobic modification on carbon dioxide absorption using porous alumina (Al2O3) hollow fiber membrane contactor', *J. Membr. Sci.*, vol. 518, pp. 79–87, Nov. 2016.
[34] A. Dupuy, 'Stabilisation de l'inerface liquide-liquide dans un contacteur membranaire : application à l'extraction sélective de terpènes oxygénés d'huiles essentielles d'agrumes', AgroParisTech, 2010.
[35] A. Sengupta, P. A. Peterson, B. D. Miller, J. Schneider, and C. W. Fulk Jr, 'Large-scale application of membrane contactors for gas transfer from or to ultrapure water', *Sep. Purif. Technol.*, vol. 14, no. 1, pp. 189–200, 1998.

[36] R. Sander, ‘Compilation of Henry’s law constants, version 3.99’, *Atmospheric Chem. Phys. Discuss.*, vol. 14, no. 21, pp. 29615–30521, Nov. 2014.
[37] J.-G. Lu, Y.-F. Zheng, and M.-D. Cheng, ‘Wetting mechanism in mass transfer process of hydrophobic membrane gas absorption’, *J. Membr. Sci.*, vol. 308, no. 1–2, pp. 180–190, Feb. 2008.
[38] J.-G. Lu, Y.-F. Zheng, and M.-D. Cheng, ‘Membrane contactor for CO2 absorption applying amino-acid salt solutions’, *Desalination*, vol. 249, no. 2, pp. 498–502, Dec. 2009.

7 ACKNOWLEDGEMENTS

- This work was financially supported by the Marne departmental council, the Champagne-Ardenne regional council and Reims Metropole through the Biotechnology Chair of CentraleSupelec.